buildings

MDPI

Article

Study on the Correlations Between Spatial Morphology Parameters and Solar Potential of Old Communities in Cold Regions with a Case Study of Jinan City, Shandong Province

Fei Zheng, Peisheng Liu, Zhen Ren, Xianglong Zhang, Yuetao Wang * and Haozhi Qin

School of Architecture and Urban Planning, Shandong Jianzhu University, Jinan 250101, China; 12914@sdjzu.edu.cn (F.Z.); 19707086531@163.com (X.Z.)
* Correspondence: wyeto@163.com

Abstract: Currently, urban development has entered the stage of renewal and transformation. Energy transition is an important trend for sustainable urban development, and the assessment of solar energy potential in old residential areas in cold regions is of great significance. This study selects 47 old residential communities in Jinan, a cold region of China, as case samples. Using clustering algorithms based on spatial form characteristic parameters, the study divides the samples into five categories. The study then uses the Ladybug tool to simulate the distribution and total solar energy utilization potential of buildings in the five categories and analyzes the correlation between eight spatial form parameters and building solar energy potential. A linear regression model is established, and strategies for the application of BIPV in community buildings are proposed. The study finds that factors such as plot ratio, building density, open space ratio, volume-to-surface ratio, and form coefficient have a significant impact on the solar energy potential of residential communities; the *p*-values are −0.785, −0.783, 0.783, −0.761, and 0.724, respectively. Among these, building density (BD) is the most crucial factor affecting the solar energy potential of building facades. Increasing by one unit can reduce the solar energy utilization potential by 28.00 $kWh/m^2/y$. At the same time, installing photovoltaic panels on old residential buildings in cold regions can reduce building carbon emissions by approximately 48%. The research findings not only provide methodological references for photovoltaic technology application at varying neighborhood scales in urban settings but also offer specific guidance for low-carbon retrofitting of aging urban communities, thereby facilitating progress in urban carbon emission reduction.

Keywords: cold regions; old communities; BIPV; spatial morphology; correlation analysis

check for updates

Academic Editor: Francesco Reda

Received: 12 March 2025
Revised: 7 April 2025
Accepted: 8 April 2025
Published: 10 April 2025

Citation: Zheng, F.; Liu, P.; Ren, Z.; Zhang, X.; Wang, Y.; Qin, H. Study on the Correlations Between Spatial Morphology Parameters and Solar Potential of Old Communities in Cold Regions with a Case Study of Jinan City, Shandong Province. *Buildings* **2025**, *15*, 1250. https://doi.org/10.3390/buildings15081250

1. Introduction

With economic development and population growth, the world is experiencing a wave of rapid urbanization. Global energy demand is increasing, which has led to an energy crisis and climate change. Carbon emissions are receiving increasing attention worldwide. The world's energy choices are shifting towards sustainable development and cleaner energy utilization methods. Human activities in cities are a significant source of greenhouse gas emissions, and residential buildings, as essential spaces for human production and daily life, occupy a substantial portion of urban areas. During the rapid economic development of China in the 1980s and 1990s, a large number of residential buildings were constructed. After three to four decades of use, these buildings no longer meet the current needs of residents.

Currently, there are approximately 170,000 old and dilapidated residential communities, accounting for about 12% of the total existing residential buildings in the country [1]. Among them, the proportion of old residential areas in major cities in China's cold areas is shown in Figure 1. As an important component of urban residential buildings, they have attracted significant attention due to their low-carbon and energy-saving renovation [2]. The old residential communities in urban China generally have the characteristics of high building density and high utilization intensity [3]. Optimizing urban spatial morphology is of significant importance in reducing building carbon emissions [4]. From the perspectives of scale and utilization intensity, installing photovoltaic systems on old urban residential buildings has significant potential to reduce building carbon emissions. In recent years, the photovoltaic power generation and its proportion in the total electricity consumption of Shandong Province are shown in Figure 2. Currently, research on building solar energy utilization mainly focuses on three levels: urban, district, and individual buildings. Urban building solar energy utilization is an important strategy for cities to promote renewable energy use [5]. Scholars have conducted research on this topic from various dimensions and perspectives. For example, technologies such as aerial photography or LiDAR (light detection and ranging) are used to identify urban buildings and other objects in order to obtain high-precision digital terrain models (DTMs) and digital surface models (DSMs). This enables 3D modeling of the entire city, allowing for the rapid calculation of solar radiation at the urban scale and the analysis of the solar energy utilization potential of rooftops.

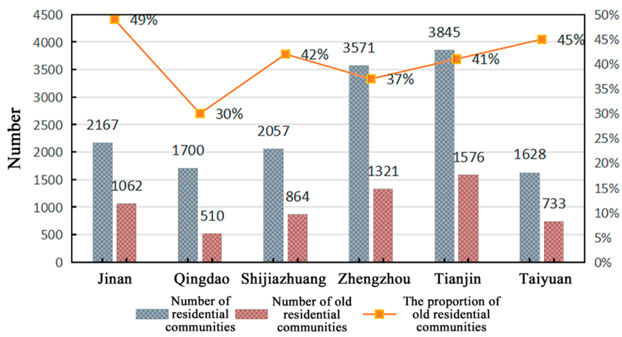

Figure 1. The proportion of old residential areas in major cities in cold areas.

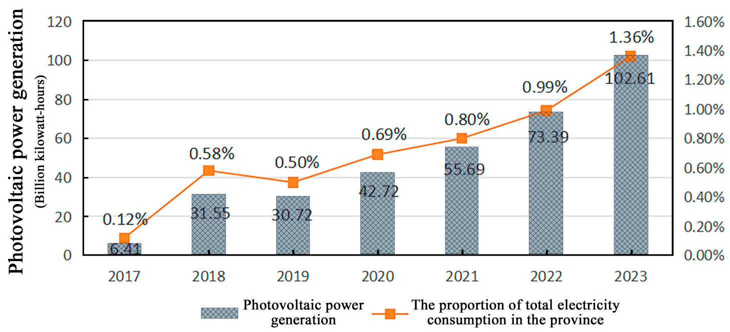

Figure 2. 2017–2023 photovoltaic power generation and its proportion in Shandong Province.

In addition, to explore the relationship between spatial morphology parameters and the solar energy utilization potential of buildings, scholars have conducted research on the solar energy potential at the block level from various perspectives. Z. Y. Fan and others simulated the energy generation of building-integrated semi-transparent photovoltaics in 14 climate representative cities and found that the solar energy utilization potential varies with the climate of each city [6]. K. S. Lee and others used computer simulations to investigate the impact of various design factors, such as building type, site coverage ratio, and floor area ratio, on solar energy utilization potential. They also employed multiple linear regression to analyze the relationship between solar energy and building layout [7]. M. Morganti and others identified correlations between building solar energy utilization and urban morphology indicators (UMIs), including the overall spatial index, facade-to-space ratio, and sky factor. Their research highlighted how these spatial characteristics influence the solar energy potential of buildings [8]. A. Vulkan and others studied the photovoltaic potential of rooftops and facades in high-density urban residential areas, focusing on the impact of nearby building shading. They assessed how shading affects the solar energy potential of rooftops and facades and analyzed the extent to which these surfaces contribute to the overall solar energy potential of the city's buildings [9]. S. Xu and others used clustering algorithms to classify 48 urban industrial districts into 7 categories, calculated the solar energy distribution and total potential of the districts, and proposed photovoltaic optimization strategies. The results show that building density has the greatest impact on building solar energy potential [10]. These studies indicate a close relationship between urban spatial morphology and the solar energy utilization potential of residential buildings [11,12]. Determining their correlation can better assist architects in developing photovoltaic installation strategies and promote the sustainable development of urban energy.

As mentioned above, although the relationship between spatial morphology parameters and solar energy utilization potential has been widely studied, most research focuses on solar energy utilization at the urban and individual building levels. Studies on solar energy potential in residential buildings at the district scale are mostly concentrated in Europe and the United States. Due to regional and national differences, the spatial morphology patterns of residential buildings in foreign countries differ significantly from those in China [13]. As a result, the findings from these studies may not be directly applicable to residential communities in China. Current research in China on the solar energy potential of aging urban residential communities is insufficient. Most studies rely on remote sensing images combined with machine learning algorithms or use GIS to estimate the solar energy potential of building rooftops within cities. However, these methods are not suitable for studying the solar energy potential of Chinese residential communities, which have regular patterns in their urban spatial morphology.

In residential communities in China, rooftops are not the only locations for photovoltaic (PV) installations. The building envelope (facade and walls) can also serve as an implementation path for building-integrated photovoltaics (BIPV). However, it is more susceptible to shading effects from adjacent buildings and other environmental factors, which can reduce the energy output of the photovoltaic system [14]. Affected by the angle of solar incidence and environmental shading, although photovoltaic systems on vertical facades receive less solar radiation compared to rooftops, the large surface area of residential building facades means that integrated photovoltaic systems on these facades can still make a significant contribution to the low-carbon and energy-saving development of urban buildings [15]. Although photovoltaic applications have broad prospects, factors such as urban geographical location, building orientation, roof type, and surrounding obstacles can all affect the efficiency of photovoltaic energy utilization. This necessitates the study of solar energy potential at the street and block scale in complex urban environments.

Therefore, this study will focus on the impact mechanism of the spatial form parameters of old residential areas on solar energy utilization potential in cold regions. Through quantitative analysis, it aims to reveal the role of the block level in the urban spatial solar energy utilization potential. In Jinan, a city in China's cold regions, 47 samples were selected based on the community layout, morphological parameters, and roof types and grouped into five categories using cluster analysis as research subjects. Using numerical simulation methods, the solar energy utilization potential of different sample types was calculated, and the impact of urban spatial form parameters on solar energy utilization potential was analyzed.

Compared to other studies, this research focuses on old residential communities in cold regions. It systematically evaluates the photovoltaic potential of roofs and façades, addressing the characteristics of high-density housing in China. The study finds that the photovoltaic potential of facades has been severely underestimated, breaking through the previous limitation of only focusing on roofs. Additionally, a multidisciplinary approach was employed to quantify the relationship between eight spatial form parameters and solar energy potential for the first time, creating a high-precision predictive model. Finally, differentiated photovoltaic strategies (such as prioritized façade installation for tower-type buildings) are proposed, and their carbon reduction benefits are verified, providing localized solutions for low-carbon renovation of old residential communities in cold regions.

2. The Full Simulation

2.1. Study Area

The study selected Jinan, Shandong Province, China, as the research area. Jinan is located in the central-western part of Shandong Province, China, at the transitional zone between the Lu Zhong Mountain Range and the Lu Xibei Plain. Its geographical coordinates are 36°02′–37°54′ N and 116°21′–117°93′ E. To the east, it borders Zibo; to the south, it adjoins Tai'an; to the west, it connects with Liaocheng; and to the north, it is close to Dezhou and Binzhou. The Yellow River flows through the city from southwest to northeast. The southern part of the city is characterized by low hills and mountains formed by the Tai Mountain range, while the northern part is a Yellow River alluvial plain, with the terrain being higher in the south and lower in the north. As the capital of Shandong Province, Jinan is a transportation hub connecting the East China and North China regions, and it features both mountainous landscapes and flat plain geography.

Jinan is classified as a cold region in China's building thermal design zones. Jinan has a temperate monsoon climate, with abundant sunlight throughout the year. The annual average sunshine duration is approximately 2400 h. In summer (June to August), the sunlight lasts the longest, with an average of about 230 h per month. In winter (December to February), the sunlight duration is shorter, with an average of about 170 h per month. The annual average wind speed is about 2.5 m per second, with stronger winds in spring (March to May), averaging about 3 m per second per month, and weaker winds in summer and autumn. The annual average temperature is around 14.5 °C, with July being the hottest month (around 27 °C) and January the coldest (around −1 °C). The region has a significant demand for energy in building heating and cooling [16]. Precipitation is concentrated in summer, while winter is dry and cold. Spring and autumn are mild and pleasant.

Therefore, the region has a significant energy demand for building heating and cooling. Jinan receives an annual solar radiation of 1376 kWh/m^2 and has an annual sunshine duration of 2542.7 h, indicating an abundant solar energy resource. As the capital city of Shandong Province, Jinan experienced rapid economic development from the 1980s onwards, with the concurrent construction of multi-story residential neighborhoods to meet the needs of population growth and urban development. The majority of the multi-story neighborhoods in the central area of Jinan were built in the early and middle 1990s. The study selected the built-up area of the city center of Jinan as the research area, where the intensity of urban development is generally higher due to the longer construction history. The research area comprises a mixture of residential neighborhoods, commercial areas, business centers, and urban villages, resulting in various limitations for photovoltaic installations.

2.2. Method

The study employed a block type-based approach to analyze the samples and their surrounding environments. The geometric shapes of the samples and the built urban environments surrounding them were used to categorize them based on density, building layout, and other characteristics. The 3D model used in the study was created in the Rhino 8.0 (non-open source) modeling software, and the spatial form parameters were calculated using QGIS 3.36 (open source) and Grasshopper 2.0 (non-open source). The solar radiation received by the sample was calculated using the Ladybug Tools1.3 (open source) plugin integrated into the Grasshopper platform.

Compared to other software, Ladybug is deeply integrated with Grasshopper and supports parametric building environment simulation and multidimensional visual analysis, making it suitable for sustainable design optimization of architectural schemes. Its built-in Radiance and EnergyPlus engines allow for the customization of building envelopes and surrounding environment parameters to calculate the direct and indirect solar radiation received by the building's surfaces. Based on the calculation results, the spatial form parameters' correlation with solar energy utilization was analyzed using the R 4.4.3 and RStudio 1.1 (open source) statistical analysis software. Stepwise selection was then applied to retain the most significant parameters for multiple linear correlation analysis, which was used to establish a regression calculation model.

In the first stage, 47 samples of old communities were selected based on the surrounding built environment and geographical location. High-resolution satellite images and 2D building footprints were obtained from sources such as OpenStreetMap (open source). On-site investigations were conducted to determine the number of floors, facade characteristics, and surrounding environmental elements of the buildings. The building height was estimated based on the average floor height (3 m), the urban form of the building was constructed using geometric blocks around the target, and the site's building 3D data was extracted and imported into Rhino for constructing a sample 3D geometric model [17,18]. (The standard floor height of common residential buildings is typically between 2.8 and 3.2 m, so 3 m was selected as the average floor height.)

In the second stage, based on the investigations and surveys conducted in the research area, the composition logic and spatial design parameters of the sample neighborhoods were determined. The impact of surrounding buildings on the sample neighborhoods in terms of shading and other factors was investigated, and the influencing factors of spatial form were recorded. The samples were classified into five types using clustering analysis as the classification criterion. The consideration of shading is to account for the real-world scenario where other buildings around urban old communities impact their reception of solar radiation. Determining the surrounding impact can provide guidance for subsequent practical calculations of building photovoltaic layouts. Additionally, the calculation of some morphological parameters in subsequent steps may be affected by the environment; however, this will not ultimately impact the research results.

In the third stage, the areas suitable for photovoltaic utilization within the sample neighborhoods were identified. Ladybug Tools [19], a plugin integrated into the Grasshopper platform, was used to import typical meteorological year (TMY) data for solar radiation simulation on a 1×1 m grid on building surfaces. The solar radiation received by each test block was calculated, and it was determined whether the cumulative solar radiation exceeded the standard test conditions of photovoltaic panels. The photovoltaic power generation capacity was then statistically analyzed.

In the fourth stage, the correlation between spatial morphology parameters and photovoltaic power generation capacity was analyzed. The relationship between the photovoltaic power generation capacity per unit area of the sample facades and spatial form was visualized using scatter plots and correlation heatmaps. A linear regression model was established, and application strategies were proposed. The workflow of this study is shown in Figure 3.

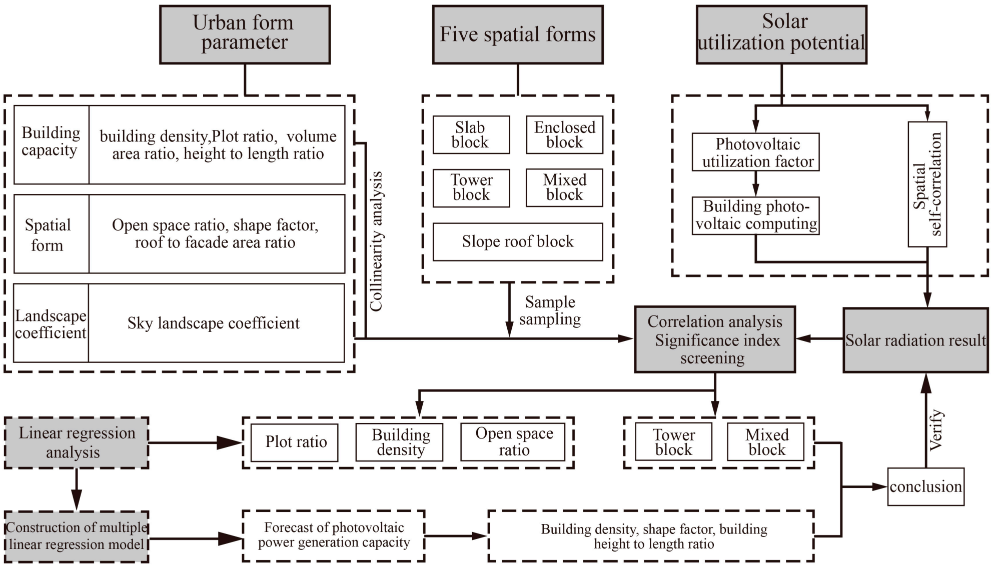

Figure 3. Flow of the study.

2.3. Morphological Parameters and Sample Extraction

The spatial form of urban residential neighborhoods determines the shading pattern between buildings, thus affecting the solar energy utilization potential of the entire neighborhood. The layout of street blocks and residential neighborhoods is controlled by various urban spatial morphology parameters. Based on the literature review, this study selects control indicators that cause shading and obstruction to buildings, including volume-area ratio (VA), floor area ratio (FAR), building density (BD), open space ratio (OS), shape factor (SF), roof-to-facade area ratio (RF), building height-to-length ratio (HLR), and skyline view factor (SVF). SVF refers to the ratio of the solid angle of visible sky to the entire sky dome, which is directly related to the use of solar energy on facades and is determined by the position and form of the surrounding buildings, which determines obstacles to direct and indirect solar radiation. After setting up the sample models in Grasshopper, the parameter tool was used to calculate the respective urban form control parameters. Table 1 lists the meanings and calculation formulas of the form parameters.

Sample Selection Criteria

(1) Selection criteria for buildings: The selected samples primarily consist of residential communities built between 1980–2000 in Jinan. During this period, the neighborhoods predominantly adopted robust brick-concrete or frame structures, with 72% featuring flat or slightly sloped roofs—ideal conditions for PV installation. Architecturally, these buildings exhibit favorable characteristics including wider building spacing (12–15 m) and regular roof shapes (92% rectangular), achieving an average usable roof area ratio of 65%, significantly higher than modern communities. Furthermore, this period's residential buildings avoided complex decorative components and reserved ample space for equipment (4–6 m^2 per unit), and the layout of the pipelines was more conducive to photovoltaic integration, creating a unique advantage for solar energy utilization.

Table 1. Urban form parameters.

Morphological Parameter	Computational Equation	Schema	Morphological Parameter	Computational Equation	Schema
Volume-Area Ratio (VA)	$VA = \frac{\text{Total building volume}}{\text{Site area}}$	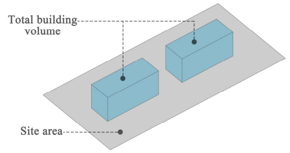	Shape Factor (SF)	$SF = \frac{\text{Building Exterior Area}}{\text{Construction Volume}}$	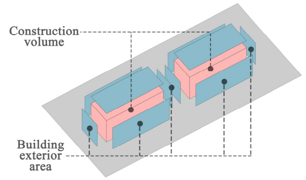
Floor Area Ratio (FAR)	$FAR = \frac{\text{gross floor area}}{\text{Site area}}$	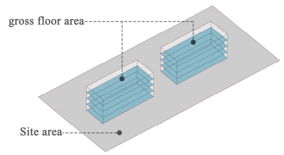	Roof-To-Facade Area Ratio (RF)	$RF = \frac{\text{Roof Area}}{\text{Enclosure Area}}$	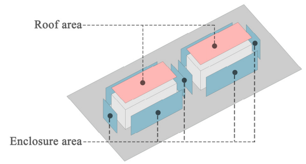
Building Density (BD)	$BD = \frac{\text{Total area of the base}}{\text{Site Area}}$	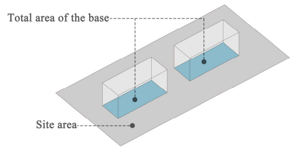	Building Height-To-Length Ratio (HLR)	$HLR = \frac{\text{Average Building Height}}{\text{Average Length Of Buildings}}$	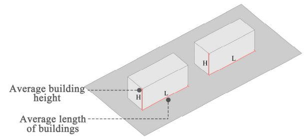
Open Space Ratio (OS)	$OS = \frac{\text{Area of open space on the site}}{\text{Site Area}}$	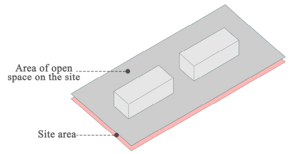	Skyline View Factor (SVF)	Obtained through the ladybug plugin sky mask component	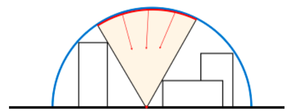

(2) Geographic location: Based on the geographical locations of sampled old communities, areas range from the early developed central urban areas to the outskirts of the city. Stratification criteria are determined based on geographical features such as the presence of building obstructions nearby, and old communities are selected and classified accordingly based on these criteria.

(3) Spatial scale: Based on the research objectives and resource constraints, the selection of sampled old communities should be based on the number of buildings and floor levels to determine the spatial scale. Sampled communities should consist of more than two buildings and be higher than three floors to ensure the representativeness of the sample.

(4) Spatial form: The zoning criteria are determined based on factors such as the building form and layout of the community. The old residential areas can be classified into slab-type, enclosed-type, tower-type, and mixed-type based on the floor plan differences, as shown in Figure 4. Finally, through cluster analysis, the selected samples within the area are divided into four categories, and parametric modeling is conducted based on the survey data, as shown in Table 2.

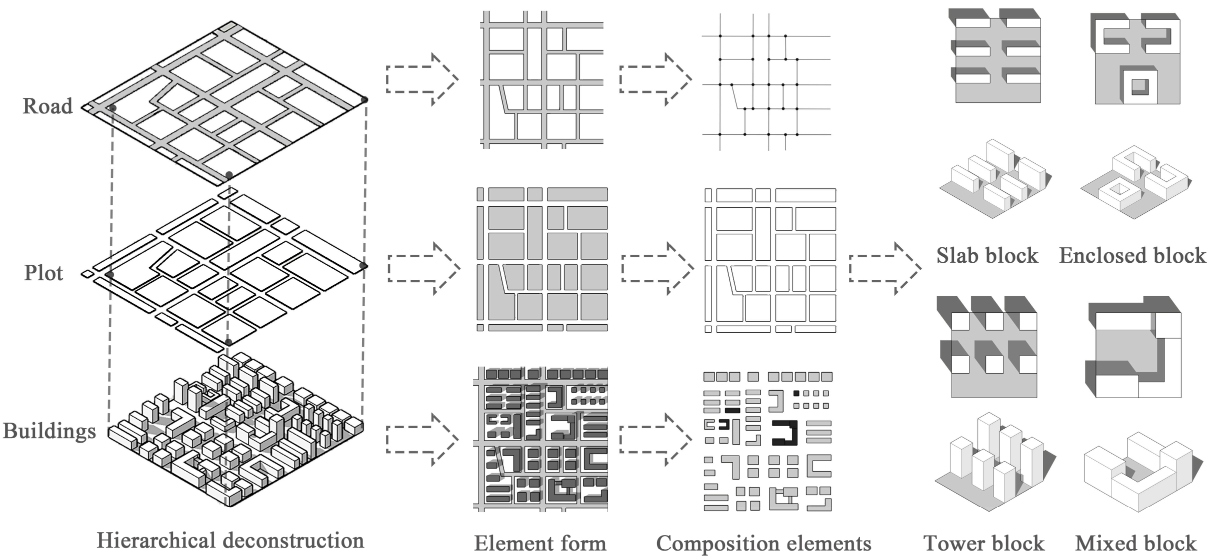

Figure 4. Division of spatial form of old residential areas in the region.

(5) Roof form: In the old residential areas of cold regions in China, the building roof types are mainly divided into flat roofs and pitched roofs, with flat roofs being more common. The sample size is determined based on the proportion of old residential areas within the region, and the final spatial form parameter results of the sample communities are shown in Figure 5.

Table 2. Clustering analysis of spatial morphology of old communities in the region.

Slab Block			Enclosed Block			Tower Block			Mixed Block		
No.	**Location Map**	**Model Diagram**	**No.**	**Location Map**	**Model Diagram**	**No.**	**Location Map**	**Model Diagram**	**No.**	**Location Map**	**Model Diagram**
A-1			B-1		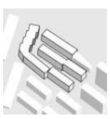	C-1		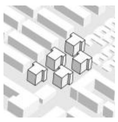	D-1		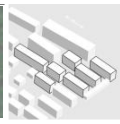
	First Dormitory (1990)			Wangguanzhuang District 1 (1996)			Bijiawa West Community (1990)			147 Wei'er Road (1996)	

Table 2. *Cont.*

No.	Slab Block Location Map / Model Diagram	No.	Enclosed Block Location Map / Model Diagram	No.	Tower Block Location Map / Model Diagram	No.	Mixed Block Location Map / Model Diagram
A-2	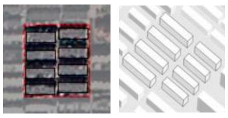 Zi Xiang Yuan (1998)	B-2	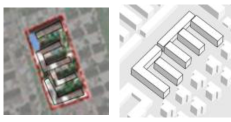 Qili Mountain South Village, Section 4 (1990)	C-2	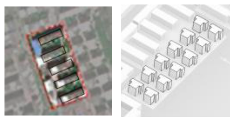 Qili Mountain South Village, Section 4 (1986)	D-2	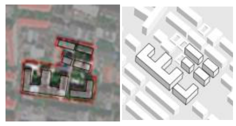 Zhi Jin Shi Community (1996)
A-3	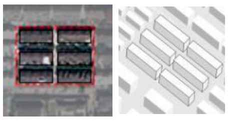 Ma Jia Zhuang Dormitory (1990)	B-3	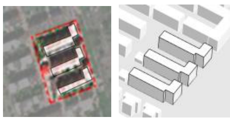 Qili Mountain South Village, Section 3 (1985)	C-3	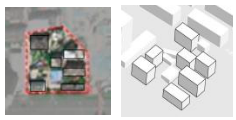 Cement Factory Dormitory (1990)	D-3	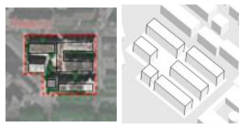 Zhengjue Temple Community, Section 3 (1992)
A-4	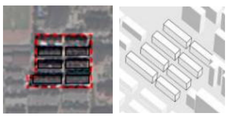 Dongyuan Community (1999)	B-4	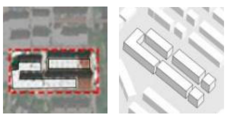 Shifan Community South Area (1993)	C-4	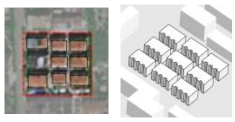 Jinan TV Station Dormitory (1999)	D-4	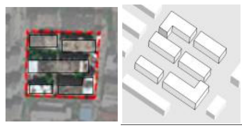 Baotu Spring Community (1992)
A-5	 Jinan Municipal Construction Committee Dormitory (2000)	B-5	 Minghu Community East District, Section 4 (1999)	C-5	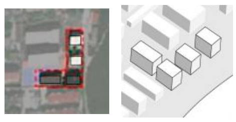 Shandong Provincial Radio and Television Department Dormitory (1999)	D-5	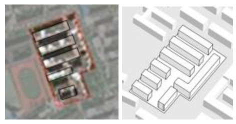 Qilishan South Village, Section 2 (1992)
A-6	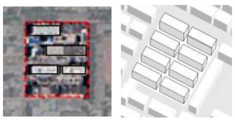 Erqi Chenzhuang (1992)	B-6	 Minghu District East District 1 (1990)	C-6	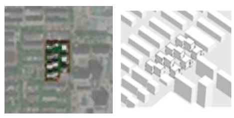 District 2, Dianliu New Village (1990)	D-6	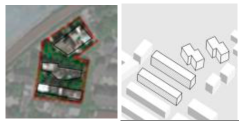 Chenjialou Community (1987)
A-7	 Yiyuan Community (1992)	B-7	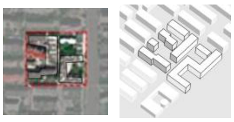 Zhengkyosi Community (1994)	C-7	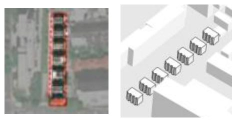 Provincial Economic and Information Commission Dormitory (1998)	D-7	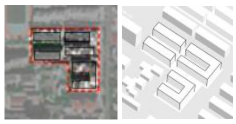 Hongtai Community (1992)
A-8	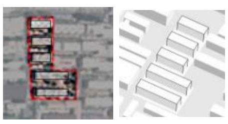 Jianxing Community (1998)	B-8	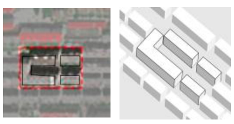 Erqi New Village District 1 (1990)	C-8	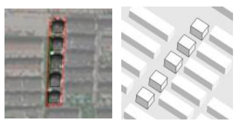 Wangguanzhuang District 8 (1996)	D-8	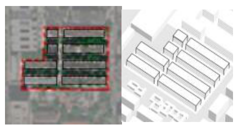 Shandong Provincial People's Government Dormitory (1985)

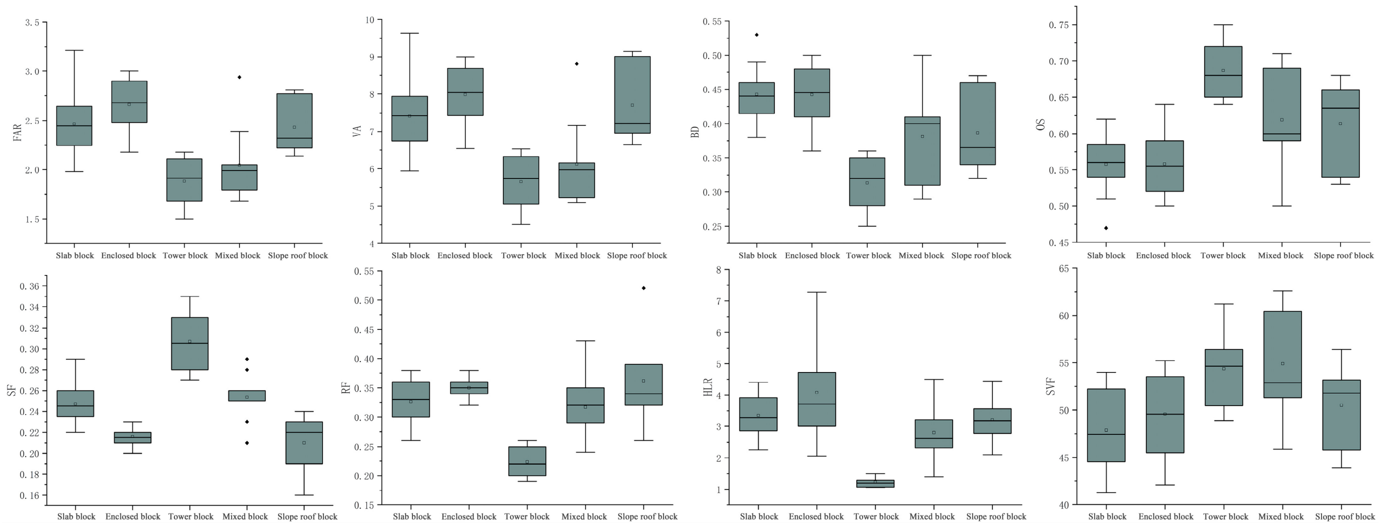

Figure 5. Sample cell spatial morphology parameter results.

2.4. Building PV Calculations

2.4.1. Photovoltaic Utilization Factor

The photovoltaic utilization coefficient refers to the ratio of the remaining surface area available for photovoltaic installation to the total building surface area, excluding factors such as windows and structural components. By analyzing whether the solar radiation falling on the building surface exceeds the solar radiation threshold required by the photovoltaic components, the feasibility of installing photovoltaic modules at that location can be determined. Therefore, in this study, the effective coefficient of roofs (C_r) and facades (C_f) will be determined based on the sampled communities.

$$C_r = C_{ro} \times C_f \times C_{st} \times C_p \times C_e \quad (1)$$

$$C_f = C_{sf} \quad (2)$$

In Equation (1), C_{ro} represents the roof area coefficient, which is the ratio of the roof area to the building area, with a value of 0.9. C_f represents the facility coefficient, which refers to the proportion of the roof not occupied by HVAC equipment, chimneys, etc., with a value of 0.8. C_{st} represents the solar water heater coefficient, which refers to the proportion of the roof not occupied by solar water heating systems, set at 0.9. C_e represents the roof utilization coefficient, with a value of 1 for flat roofs and 0.69 for sloping roofs.

If the building is a regular rectangle with no complex shape, the roof area may be close to the footprint area. However, in practice, some edge space is often left out (such as for gutters and railings), so a roof area ratio of 0.9 is more reasonable. Residential buildings usually need to place equipment such as cooling towers, fans, and pipes on the roof, which may occupy 15–25% of the roof area, so the facility ratio is typically 0.8. Solar collectors usually cover part of the roof, with coverage often around 10%, so the solar water heater ratio is generally 0.9. For flat roofs, the entire projected area can be directly used to install equipment or photovoltaic panels. The pitch of sloped roofs is typically between 30° and 45°, and the roof utilization ratio generally ranges between 0.71 and 0.87 (cos45°–cos30°). However, considering the structural limitations of the ridge line, eaves, and other features of the sloped roof, the roof utilization ratio is typically selected as 0.69.

In Equation (2), C_{sf} represents the facade equipment coefficient, which is the ratio of the area not occupied by air conditioning facilities to the facade area, excluding windows, set at 0.9. The building height is uniformly set at 3 m. The window-to-wall ratio for the south facade is 0.35, and there are no windows on the east and west facades. The height of the windows above the ground is 1.1 m for each floor.

2.4.2. Photovoltaic Potential

The comparison table of common photovoltaic module parameters is shown in Table 3. Compared to monocrystalline silicon, polycrystalline silicon is more affordable. Based on current mainstream trends and comprehensive considerations, the study adopts polycrystalline silicon photovoltaic modules with the following specifications: 380 W power output, dimensions of 1650 × 992 × 40 mm, and a weight of 20 kg per panel.

Table 3. Comparison table of common photovoltaic module parameters.

Type	Power (W)	Size (mm)	Weight (kg)	Efficiency (%)	Manufacturer
Monocrystalline silicon (PERC)	400–450	1754 × 1096 × 30	19–22	20–21.5	LONGi Green Energy from Xi'an, China
Monocrystalline silicon (TOPCon)	420–480	1762 × 1134 × 30	21–23	21–23	Jinko Solar from Jiangxi, China
Polycrystalline silicon	350–380	1650 × 992 × 40	18–20	15–17	Tongwei Group from Sichuan, China
Thin film (CdTe)	350–420	1200 × 600 × 6.5	12–15	15–18	LONGi Solar CdTe from Hangzhou, China

This study calculates the building photovoltaic utilization coefficient and further estimates the photovoltaic installation ratio on each surface of the building, which represents the proportion of available area for photovoltaic modules on each building surface. The calculation formulas are as follows:

$$R_{roof} = \frac{P_{roof}}{A_{roof}} \tag{3}$$

$$R_{facade} = \frac{P_{facade}}{A_{facade}} \tag{4}$$

Equations (3) and (4) represent the photovoltaic installation ratios on the roof (R_{roof}) and facade (R_{facade}) of the building, respectively. P_{roof} and P_{facade} represent the available areas for photovoltaic installation on the roof and facade, while A_{roof} and A_{facade} represent the total areas of the roof and facade. The available photovoltaic area is determined by samples obtained, primarily influenced by the radiation threshold of photovoltaic panels. The radiation threshold refers to the minimum radiation required for photovoltaic panels to achieve a balance between energy generation and consumption over their entire lifespan. In this study, the threshold for rooftop solar photovoltaic generation is set at 486 kWh/m^2/y.

The solar power generation potential is an important indicator for calculating the photovoltaic utilization potential of the building. The factors considered in electricity generation include the conversion efficiency of photovoltaic modules, the potential for photovoltaic installation, and the degradation rate of the components. According to the "Design Specification for Photovoltaic Power Stations" (GB 50797-2012) [20], the formula for calculating photovoltaic power generation is as follows:

$$E_P = H_A \times A_{PV} \times K \times \eta \times (1 - R_d)^{N-1} \tag{5}$$

In Equation (5), H_A represents the total annual solar radiation received by the building surfaces. A_{pv} represents the available area for installing photovoltaic modules on the building surfaces, η represents the photovoltaic conversion efficiency (set at 17.3%), K represents the comprehensive efficiency coefficient (set at 87%), R_d represents the photovoltaic module's degradation rate (set at 1.4%), and N represents the service life of 25 years.

The study calculates the solar energy utilization potential per unit building area within the samples and represents it as the photovoltaic generation intensity (PVGI), as calculated by Equation (6).

$$\mathrm{PVGI} = \frac{E_P}{A_T} \tag{6}$$

In Equation (6), PVGI is the photovoltaic generation intensity (kWh/m^2/y), E_p is the annual solar energy generation of the photovoltaic panel (kWh/y), and A_T is the total building area (m^2).

The photovoltaic power (PV Power) refers to the maximum power that a photovoltaic system can generate under specific conditions (such as a certain radiation intensity, temperature, etc.), calculated by Equation (7).

$$PV\ Power = PVGI \times A_{PV} \tag{7}$$

In Equation (7), PV Power is the photovoltaic power (kWh/y), PVGI is the photovoltaic generation intensity (kWh/m^2/y), and A_{pv} is the area of the building surface where the photovoltaic components are installed (m^2).

Taking a building as an example, a photovoltaic panel installation model was established, with the roof elevation and south elevation diagrams shown in Figures 6 and 7.

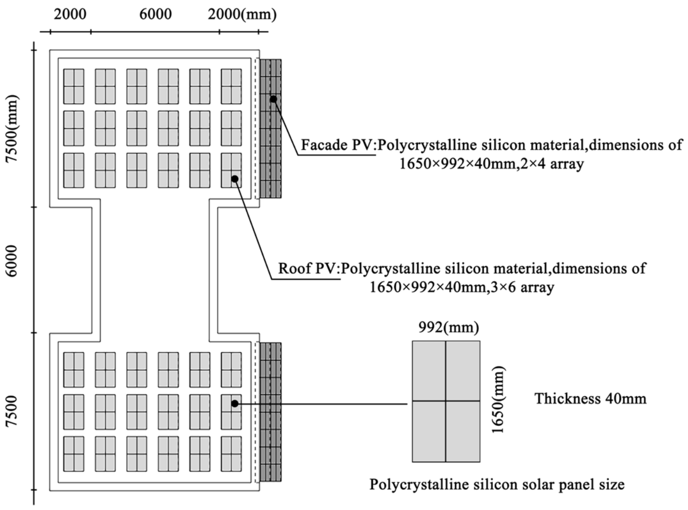

Figure 6. Roof plan of the building.

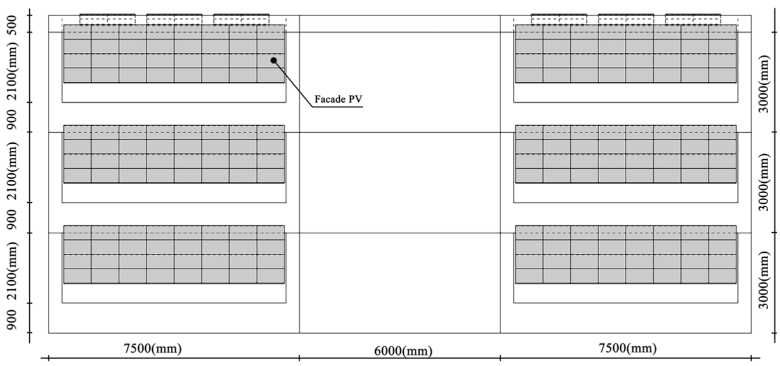

Figure 7. South elevation of the building.

3. Results

3.1. Solar Radiation Results

By conducting an annual solar radiation simulation assessment for 47 sample communities, the differences in solar radiation per square meter and distribution patterns were compared for various types of building roofs and facades in old residential areas. The study defines the annual sunshine hours as 2542.7 h.

Figure 8 shows the solar radiation received per unit building area for the samples. Through simulation and data analysis of acceptable radiation intensity for the samples, it is observed that the solar radiation received on building facades of various types exceeds that received on roofs. Among all the building types, the tower block type allows for more solar radiation to be received on the building facades. As the sample examples are located in the central urban areas, the solar radiation received on flat roofs ranges from 421.36 kWh/m^2/y to 306.76 kWh/m^2/y, with only some samples experiencing partial shading from surrounding high-rise buildings. For sloped roofs, the solar radiation received ranges from 354.03 kWh/m^2 to 256.30 kWh/m^2/y. Regarding the building facades, the average solar radiation received on the south, east, and west facades is lower than that on the rooftops. Among these, the south facade receives the most ample solar radiation due to the larger distance between buildings in the north-south direction, with a proportion above the solar radiation threshold of photovoltaic components reaching 99%. Due to mutual shading between buildings within the samples, the areas on the east and west facades that exceed the solar radiation threshold for photovoltaic components are 78% and 80%, respectively.

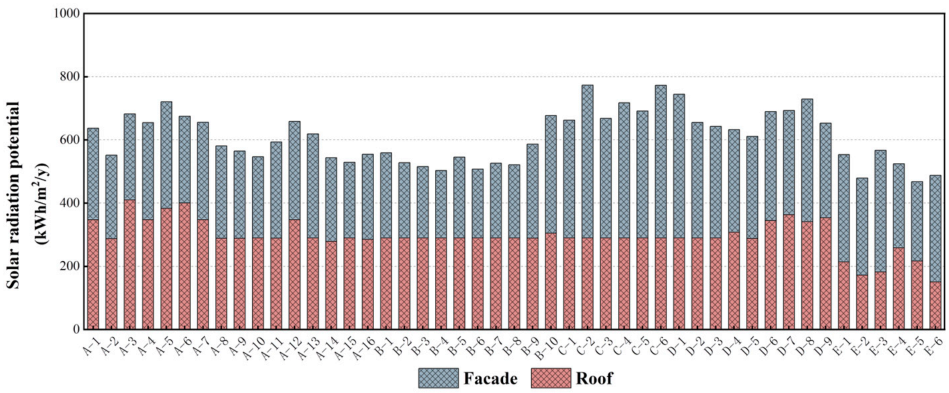

Figure 8. The illustration of the solar radiation capacity of the external facade and roof.

3.2. Intensity of Photovoltaic Power Generation

Figure 9 presents the photovoltaic generation capacity per unit building area for 47 sample units. Taking into account factors such as the installed area of photovoltaic panels on roofs and facades, photovoltaic conversion efficiency, and overall efficiency coefficients, we calculated and compared the photovoltaic generation intensity (PVGI) of different types of sample roofs and facades. The average PVGI values for the tower block and mixed block samples were significantly higher at 40.24 kWh/m^2/y and 35.87 kWh/m^2/y, respectively. The PVGI average for the slab block samples was in the middle range at 33.08 kWh/m^2/y. The enclosed block and sloped roof samples had lower and relatively similar PVGI averages at 30.56 kWh/m^2/y and 28.57 kWh/m^2/y, respectively. The difference between the highest tower block sample and the lowest sloped roof sample mean values was 11.67 kWh/m^2/y. The results show that tower Block, mixed block, and slab block samples have greater solar energy utilization potential compared to enclosed block and slope roof block samples.

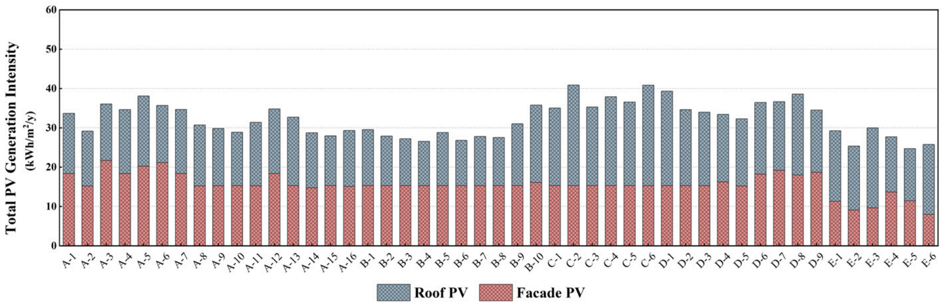

Figure 9. Schematic diagram of photovoltaic power generation intensity of rooftop photovoltaic and external facade photovoltaic.

Figure 10 presents the total photovoltaic generation intensity on the rooftops and facades of the samples. For the slab block, tower block, enclosed block, and mixed block types of residential buildings, the rooftops have similar photovoltaic generation intensities since they are all flat roofs with mostly similar-height surrounding buildings that do not cause shading. However, for the E samples with sloped roofs, the photovoltaic generation intensity on the roof is lower compared to flat roof types. In contrast to roofs, facades of different building types show significant differences in photovoltaic generation intensity due to varying layouts and surrounding building conditions.

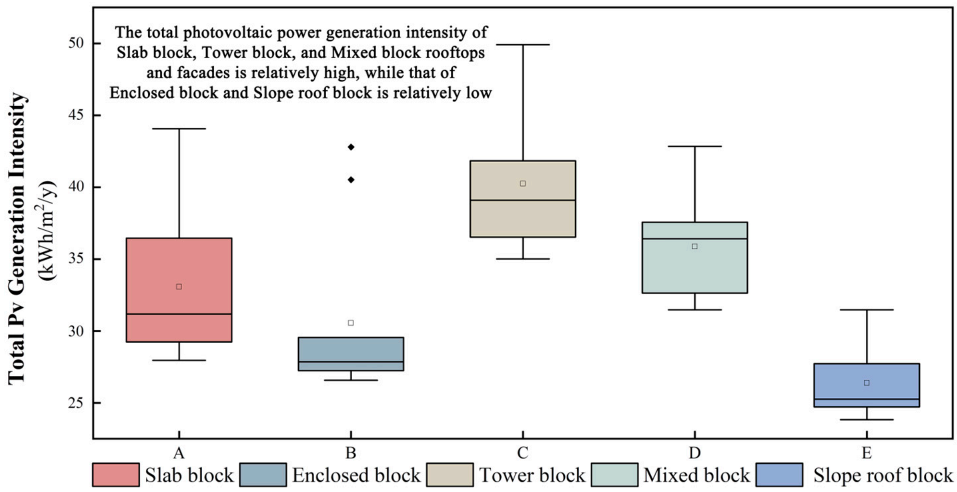

Figure 10. Box diagram of PV capacity for five sample categories.

3.3. Photovoltaic Application Strategies

Due to similar spatial layouts in communities of the same type, similar photovoltaic application strategies can be adopted. By calculating the ratio of the area on building facades and roofs that meets the photovoltaic panel irradiation threshold, multiplied by the proportion of available area for each surface, the photovoltaic installation ratio on each building surface can be obtained. From Figure 11, it can be seen that the east-facing and west-facing facades have no windows and are only affected by building shading. Their highest available area ratios are 0.69–0.76 and 0.58–0.80, respectively. The flat roof has a ratio of 0.65. The window-to-wall ratio on the south facade is relatively large, resulting in a lower usable area, ranging from 0.88 to 0.90. The sloped roof, influenced by angle and orientation, has the lowest usable area ratio at 0.48.

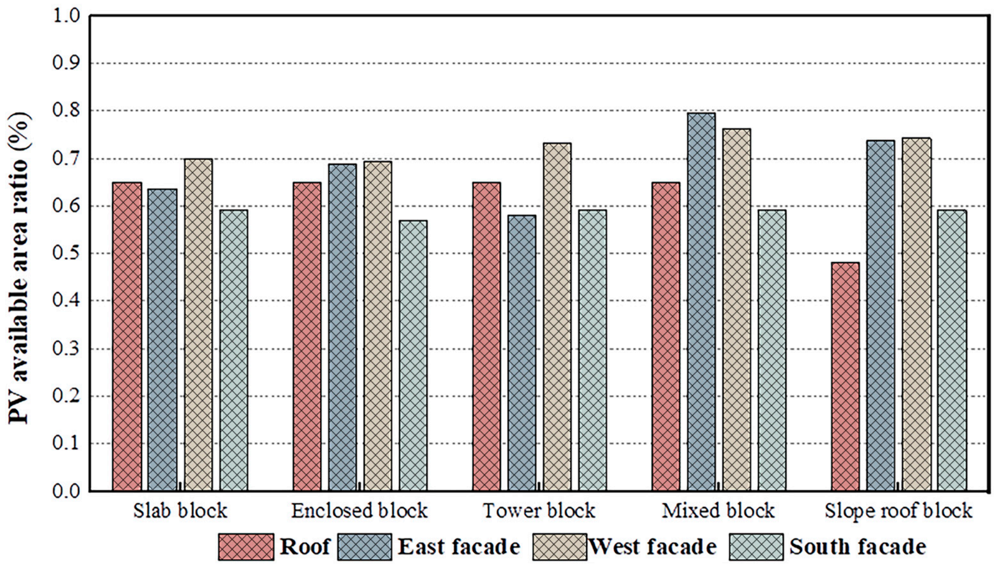

Figure 11. Ratio of PV usable area on each face of the five sample building types.

Among all the types of samples, rooftop installations have the highest proportion, featuring more concentrated areas and less impact from shadow obstruction. Compared to flat roofs, sloped roofs, although having a larger surface area, only utilize 50% of the photovoltaic area of flat roofs. The building facades are affected by the mutual shading of surrounding buildings, with facades closer to the rooftops receiving more solar radiation and facades closer to the ground receiving less. In most samples, the distance among the buildings in the north-south direction is generally equivalent to the building height, resulting in sufficient solar radiation. However, due to more windows, the usable area on the south facade is smaller than the usable area on the rooftop for photovoltaic installation. Due to the close spacing between buildings within the sample, only the higher parts of the east and west facades receive solar radiation greater than the photovoltaic threshold of 486 kWh/m^2. Almost all north facades receive solar radiation lower than the threshold. Therefore, installing photovoltaic panels on the north facades of the buildings is not considered.

4. Discussion

The differences in spatial morphology parameters result in diverse three-dimensional spatial environments in old communities and also have various impacts on the solar energy utilization potential within these neighborhoods. The variations in three-dimensional spatial environments lead to different mutual obstructions between buildings, resulting in variations in solar radiation received by building rooftops and facades, which in turn affects the overall solar potential of old communities. Therefore, this section analyzes the correlation and impact patterns between the spatial form parameters of old residential areas and the solar energy utilization potential of building facades.

4.1. Influence of Morphological Parameters on the Potential of Solar Energy Utilization

By evaluating the solar energy potential of buildings in 47 sample instances across five types of samples, the photovoltaic generation capacity of each sample neighborhood is obtained. Building upon this, the influence of different spatial morphology parameters on the photovoltaic generation capacity of building facades in old communities is investigated. Figure 12 shows the scatterplot between building facades and photovoltaic generation capacity. It can be seen that in the fitting equations of the morphological control parameters floor area ratio (FAR), volume-area ratio (VA), and building density (BD), the R^2 values are all greater than 0.50, specifically 0.62, 0.58, and 0.61, respectively. Most of the scatter points are distributed near the fitting line, indicating a strong negative correlation between FAR, VA, BD, and facade photovoltaic generation capacity. As FAR, VA, and BD increase, the overall density of the old communities also increases, leading to less solar radiation available for building facades within the community, and thus poorer facade photovoltaic generation capacity.

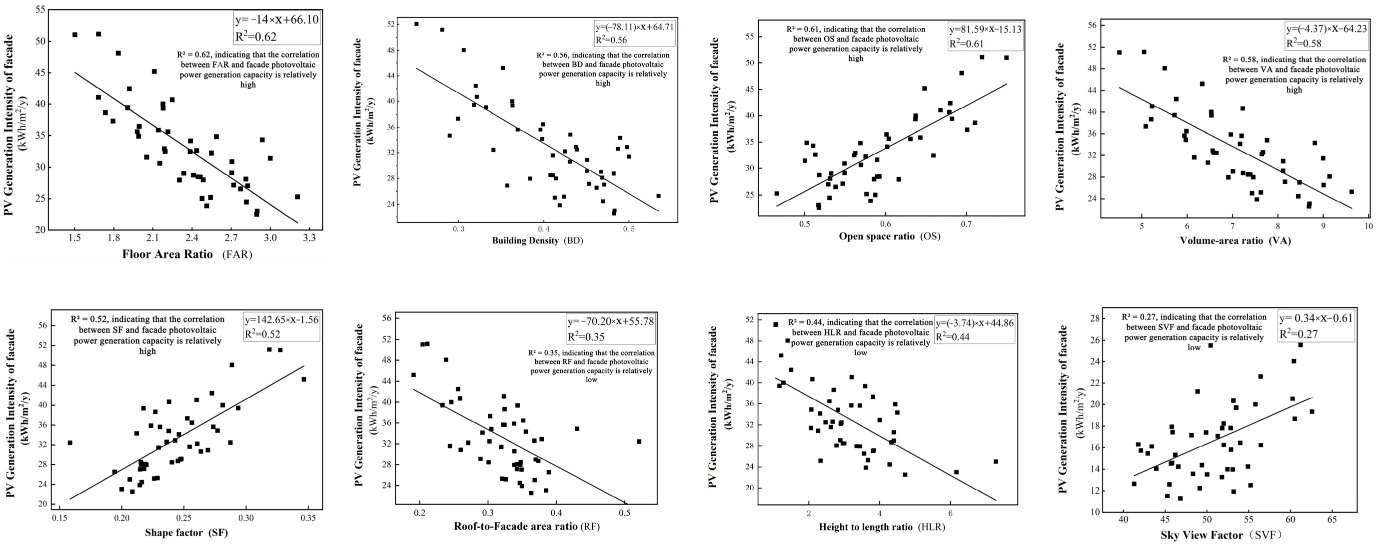

Figure 12. Scatter plot of 10 morphology parameters vs. facade PV capacity.

Similarly, in the fitting equations for open space ratio (OS) and shape factor (SF), the R^2 values are both greater than 0.50, specifically 0.61 and 0.52, and most of the scatter points are distributed near the fitting line. This indicates a strong positive correlation between OS, SF, and facade photovoltaic generation capacity. As OS and SF increase, the overall density of the old communities also increases, leading to more solar radiation available for building facades within the community and thus stronger facade photovoltaic generation capacity. However, in the fitting equations for roof-facade area ratio (RF), height-to-length Ratio (HLR), and sky view factor (SVF), the R^2 values are all less than 0.50, specifically 0.36, 0.45, and 0.27, indicating a poor fit and suggesting that RF, HLR, and SVF have a lower correlation with the facade photovoltaic generation capacity of old communities.

Upon deeper consideration, it is evident that the roof-to-facade area ratio (RF) mainly affects the allocation of photovoltaic installation surfaces but has limited impact on radiation reception. The building height-to-length ratio (HLR) only reflects the building's shape and is not directly related to external shading. Although the sky view factor (SVF) quantifies shading, the generally high density of old neighborhoods results in small SVF differences, weakening its relevance. Therefore, these three factors have weak explanatory power for facade photovoltaic power generation capacity, while parameters such as floor area ratio and building density better reflect the group shading effect.

Table 4 presents the correlation coefficient (R2) and Sig (two-tailed) values for the correlation between eight spatial morphology parameters and the facade Photovoltaic Generation Index (PVGI). Through analysis, it is observed that the parameters with the strongest correlation to PVGI are floor area ratio (FAR), building density (BD), and open space ratio (OS), with correlations of −0.785, −0.783, and 0.783, respectively. Closely following are volume-area ratio (VA), shape factor (SF), and building height-to-length ratio (HLR), with correlations of −0.761, 0.724, and −0.67, respectively. The roof-to-facade area ratio (RF) and skyline view factor (SVF) exhibit the lowest correlations, with values of −0.601 and 0.52, respectively. Among these parameters, floor area ratio (FAR), building density (BD), volume-area ratio (VA), and roof-to-facade area ratio (RF) have a negative correlation with PVGI, while open space ratio (OS), shape factor (SF), and skyline view factor (SVF) have a positive correlation.

Table 4. Regression results of solar energy utilization capacity of spatial form parameter facade.

Spatial Morphology Parameters	Pearson's Correlation Coefficient	Sig. (Two-Tailed)	R^2
Floor Area Ratio (FAR)	−0.785 **	0.00	0.62
Building Density (BD)	−0.783 **	0.00	0.61
Open Space Ratio (OS)	0.783 **	0.00	0.61
Volume-Area Ratio (VA)	−0.761 **	0.00	0.58
Shape Factor (SF)	0.724 **	0.00	0.52
Roof-To-Facade Area Ratio (RF)	−0.601 **	0.00	0.36
Building Height-To-Length Ratio (HLR)	−0.670 **	0.00	0.45
Skyline View Factor (SVF)	0.520 **	0.00	0.27

**. The correlation is significant at the 0.01 level (two-tailed).

Figure 13 shows the correlation matrix heatmap of eight spatial morphology parameters and the façade PVGI. All spatial morphology parameters exhibit a certain level of correlation with PVGI and therefore can be used as independent variables for constructing a multiple linear model. Through linear regression analysis, it is found that the VIF coefficients for FAR and VA are 35.668 and 36.765, respectively. The high correlation between these variables may increase the variance of the parameter estimates in the equation, making the prediction results meaningless. Therefore, the study will use the remaining six spatial morphology parameters as independent variables for the multiple linear regression analysis.

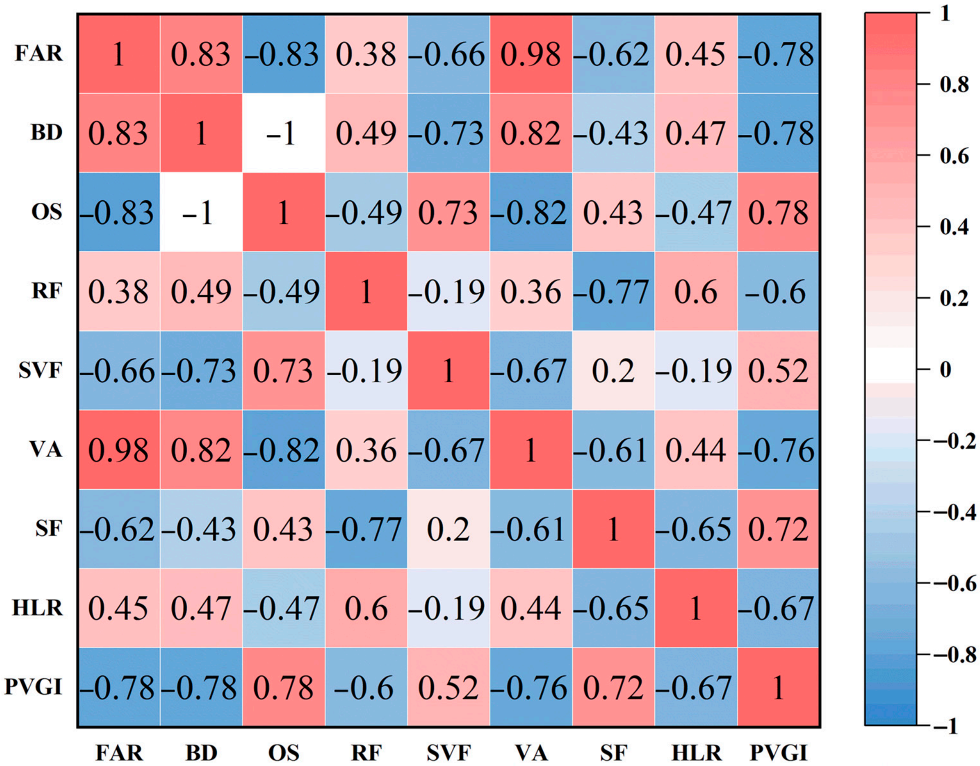

Figure 13. Heat map for correlation analysis.

4.2. Multiple Linear Regression Models for Predicting Solar Energy Utilization Potential

The correlation between individual spatial morphology parameters and the Photovoltaic Generation Index (PVGI) of building facades was calculated using correlation analysis. However, this method does not determine the comprehensive impact of multiple spatial morphology parameters on the PVGI of facades. To address this issue, this study selected six spatial morphology parameters, namely building density (BD), open space ratio (OS), shape factor (SF), roof-to-facade area ratio (RF), skyline view factor (SVF), and building height-to-length ratio (HLR). Multiple linear regression analysis was performed based on correlation analysis, employing the stepwise selection method to retain the most significant spatial morphology parameters.

Based on the model fitting degree in Table 5 and the multiple linear regression results in Table 6, it can be concluded that for all samples, BD (building density), SF (shape factor), and HLR (building height-to-length ratio) have the most significant combined impact on the facade PVGI (Photovoltaic Generation Index). The model's R^2 is 0.809, indicating that 80.9% of the variance in the dependent variable can be explained by the independent variables, demonstrating a good fit. The adjusted R^2 is 0.796, which considers the number of independent variables in the model and adjusts the value of R^2 accordingly based on degrees of freedom. The Durbin–Watson value is 1.801, indicating that the error terms are independent. The VIF values for the three independent variables, BD, SF, and HLR, are all less than 5, indicating the absence of multicollinearity issues. BD and HLR have a negative correlation with PVGI, while SF has a positive correlation with PVGI, with coefficients of −28.001, −0.490, and 37.588, respectively. An increase of 1 unit in BD would decrease PVGI by 28.00 kWh/m^2/year, an increase of 1 unit in HLR would decrease PVGI by 0.49 kWh/m^2/year, and an increase of 0.1 units in SF would increase PVGI by 37.59 kWh/m^2/year. When parameters are sorted based on standardized coefficients (beta values), BD (−0.535) has the most significant impact, followed by SF (−0.383), and HLR (−0.176). The PVGI for building facades can be calculated using Formula (8).

$$Y = 20.307 - 28.001 \times BD + 37.588 \times SF - 0.490 \times HLR \tag{8}$$

Table 5. Degree of model fit.

Model	R	R^2	After Adjusting R^2	Errors in Standard Estimates	Durbin Watson
1	0.900 [a]	0.809	0.796	1.6014	1.801

[a]. Predictor variable: (constant), HLR, BD, SF; Implicit variable: PVGI.

Table 6. Results of multiple linear regression analysis.

Model		Unstandardized Factors		Standardized Factor	t	Significance	Covariance Statistics	
		B	Standard Errors	Beta			Tolerances	VIF
1	(Constant)	20.307	3.215		6.317	0.000		
	BD	−28.001	3.995	−0.535	−7.009	0.000	0.762	1.312
	SF	37.588	8.740	0.383	4.301	0.000	0.560	1.786
	HLR	−0.490	0.254	−0.176	−1.929	0.060	0.535	1.870

Implicit variable: PVGI.

After determining the regression equation, data from 12 old residential communities in Jinan City were selected to validate its effectiveness. This dataset includes six slab block, three enclosed block, and three tower block samples, as shown in Figure 14. The average error between the measured values obtained through on-site measurements of the sample facades and the predicted values from numerical simulations is 6.02%, indicating that the prediction model is relatively accurate. This study provides valuable references for investigating the relationship between spatial form parameters and solar energy potential in old residential communities in cold regions.

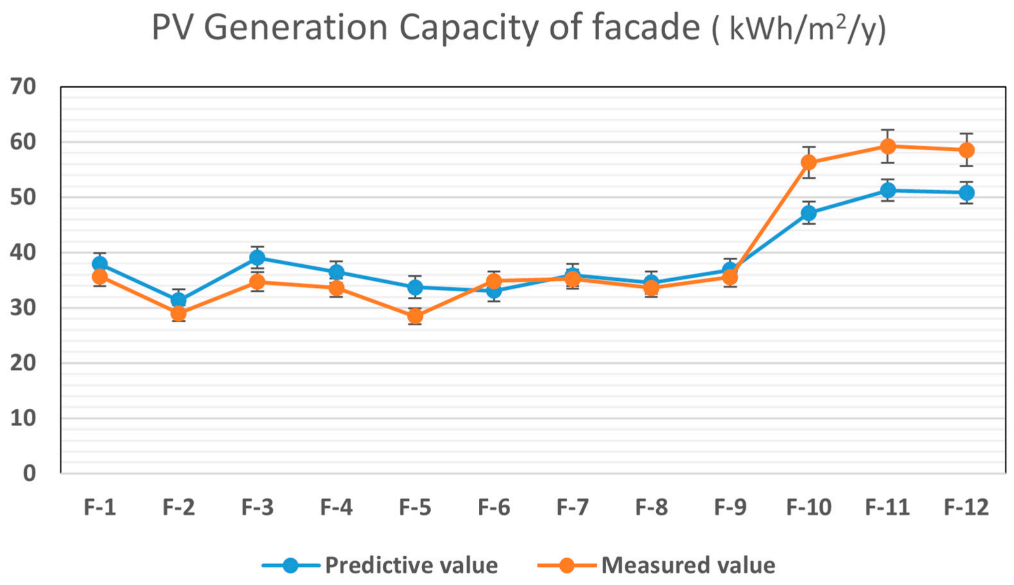

Figure 14. Comparison between measured and predicted values of facade photovoltaic generation capacity.

According to the research by Zheng, F. [21] on carbon emissions in old residential communities in cold regions, the average carbon emissions per unit area for various types of old urban residential communities in Jinan, a cold region, is 76 $KgCO_2/m^2/y$. The average solar energy utilization potential of the research samples in this study is 35.12 $kWh/m^2/y$. If photovoltaic panels are installed on both the building roofs and facades, it could reduce the carbon emissions of old residential buildings in cold regions by 47% per year.

4.3. Perspectives

Currently, the urban built environment is becoming increasingly complex, which has prompted scholars to broaden their research focus from the previous limited scope of decarbonization strategies solely related to rooftop photovoltaics to examine the impact of different spatial forms on the potential for solar energy utilization. This expansion holds significant practical significance, particularly in Chinese cities where many old communities face challenges related to high energy consumption and carbon emissions. It provides a viable pathway for carbon reduction and emission reduction efforts in cities. The validation results of this study demonstrate a strong correlation between the spatial form of old communities in urban areas and the potential for solar energy utilization in buildings. This correlation provides robust support for urban sustainable development efforts. Within these old communities, there exists tremendous potential for the utilization of solar energy in buildings. This not only helps alleviate the carbon emission pressure on cities but also provides clean energy for residents, reduces reliance on traditional energy sources, ensures the sustainability of energy supply, and enhances the quality of life. Therefore, the practical significance of this study lies in emphasizing the effective pathway of utilizing building-integrated solar energy in old communities as a means of reducing carbon emissions, particularly in cold regions. Based on the predictive model established in this research, which correlates spatial form parameters with solar energy utilization potential, cities can enhance sustainable urban development by improving building structures and integrating solar energy facilities within these communities. This approach can effectively reduce carbon emissions, enhance energy efficiency, and mitigate dependency on traditional energy sources. Furthermore, this research provides new insights for urban planning and development aimed at achieving more environmentally friendly and energy-efficient urban development goals. By promoting the findings of this research, cities can advance the utilization of renewable energy on a global scale, thereby reducing greenhouse gas emissions and contributing to solutions for climate change challenges.

5. Conclusions

This study investigated the relationship between the spatial form of old residential communities and the potential for solar energy utilization in cold regions of China from a typological perspective. It quantitatively analyzed the impact of spatial morphology parameters on the solar energy potential of old communities in Jinan, a cold region city, and discussed the distribution of solar energy utilization potential across different typologies of old residential areas. This study integrated three steps, including modeling, solar radiation simulation, solar potential calculation, and data analysis and visualization, using a customized workflow. The study evaluated the solar potential of 47 old communities using eight morphological parameters and analyzed the photovoltaic installation ratio, total photovoltaic utilization, and distribution patterns across different types of old communities. Based on the research, the following conclusions were drawn:

The photovoltaic utilization potential is highest in tower block and mixed block communities. This study shows that the average PVGI values for tower block and mixed block community samples are higher, at 40.24 kWh/m^2/y and 35.87 kWh/m^2/y, respectively, while the average PVGI value for the slope roof block community sample is lower, at 28.57 kWh/m^2/y. Therefore, future photovoltaic optimization strategies should focus on tower block and mixed block old communities, prioritizing the development of building-integrated photovoltaic (BIPV) systems for facades, along with supportive incentive policies to promote large-scale applications, in order to maximize solar energy collection efficiency and provide replicable technical pathways for urban low-carbon renewal.

Floor area ratio (FAR), building density (BD), and open space ratio (OS) have a higher impact on the photovoltaic power generation capacity of the old communities. This study performs a linear regression analysis of eight spatial form parameters and facade photovoltaic power generation capacity. The regression results indicate that the parameters most strongly correlated with facade photovoltaic power generation capacity are the floor area ratio, building density, and open space ratio, with correlation coefficients of −0.785, −0.783, and 0.783, respectively. In the future, key spatial form parameters such as floor area ratio, building density, and open space ratio should be optimized to scientifically plan the spatial layout of old residential communities, reduce shading between buildings, and improve solar radiation reception efficiency, thereby systematically enhancing the photovoltaic power generation potential and carbon reduction benefits of old communities.

The results obtained from this study can be used to assess the potential of photovoltaic power generation in cold regions based on existing data. The workflow and methods developed can serve as a reference for evaluating the photovoltaic power generation capacity of existing urban old communities in other climatic regions to determine the most effective building solar utilization designs and guidance according to the local environment. The study results also provide insights for the public and decision-makers in city administration to improve their awareness of clean energy and implement renewable energy-friendly policies.

This study still has several limitations that need to be addressed and improved in future research. The research focuses on old residential communities in Jinan, but the number of enclosed and pitched-roof old communities in Jinan is limited, which results in a relatively small sample size. Expanding the scope of the study to obtain more data samples would undoubtedly significantly enhance the practical value of the research. On the other hand, this study draws on relevant literature and practical experience to select eight spatial form parameters, including floor area ratio and building density, and constructs a database of factors influencing the spatial form of old residential communities. Although the selected parameters are somewhat representative, they are not comprehensive enough. Future research could consider incorporating additional parameters, such as community orientation and building coverage ratio, to enrich the factor database.

Author Contributions: Conceptualization, F.Z. and Y.W.; data curation, P.L. and X.Z.; formal analysis, F.Z. and Y.W.; funding acquisition, F.Z. and H.Q.; investigation, Z.R. and H.Q.; methodology, F.Z. and Y.W.; project administration, Z.R., F.Z., and Y.W.; resources, Z.R., Y.W., and H.Q.; software, P.L. and X.Z.; supervision, F.Z. and Y.W.; writing—original draft, P.L. and X.Z.; writing—review and editing, X.Z. All authors have read and agreed to the published version of the manuscript.

Funding: This research was funded by The Doctoral Research Fund Project of Shandong Jianzhu University (No. X22055Z); Shandong Provincial Natural Science Foundation General Project (No. ZR2020ME213).

Data Availability Statement: The data presented in this study are available upon request from the first author. The data are not publicly available due to privacy concerns.

Conflicts of Interest: The authors declare no conflicts of interest.

References

1. Zhang, J.; Li, M.H. Design Methods for the Protection and Renewal of Old Districts: Integration of Culture and Greenery, Symbiosis of the Old and New. *Build. Tech.* **2024**, *30*, 12–17.
2. Hui, E.C.M.; Liang, C.; Yip, T.L. Impact of semi-obnoxious facilities and urban renewal strategy on subdivided units. *Appl. Geogr.* **2018**, *91*, 144–155. [CrossRef]
3. Xie, Z.H.; Xu, Y. Research on Land Use Policies Based on Compact Urban Development. *Hous. Real Estate* **2018**, *9*, 20.
4. Wan, Z.M.; Huang, Z.L.; Zhu, J.M.; Xie, X.H. Analysis of Solar Energy Resources on Building Roofs at the Block Scale: A Case Study of Lucheng District, Wenzhou. *Green Build.* **2023**, *6*, 93–97.
5. Huang, Z.J.; Mendis, T.; Xu, S. Urban solar utilization potential mapping via deep learning technology: A case study of Wuhan, China. *Appl. Energy* **2019**, *250*, 283–291. [CrossRef]
6. Fan, Z.Y.; Xiao, Z.Y.; Liu, J.P. Energy performance assessment of semi-transparent photovoltaic integrated large-scale railway stations among various climates of China. *Energy Convers. Manag.* **2022**, *269*, 115984. [CrossRef]
7. Lee, K.S.; Lee, J.W.; Lee, J.S. Feasibility study on the relation between housing density and solar accessibility and potential uses. *Renew. Energy* **2016**, *85*, 749–758. [CrossRef]
8. Morganti, M.; Salvati, A.; Coch, H.; Cecere, C. Urban morphology indicators for solar energy analysis. In Proceedings of the 9th International Conference on Sustainability and Energy in Buildings (SEB), Chania, Greece, 5–7 July 2017; pp. 807–814.
9. Vulkan, A.; Kloog, I.; Dorman, M.; Erell, E. Modeling the potential for PV installation in residential buildings in dense urban areas. *Energy Build.* **2018**, *169*, 97–109. [CrossRef]
10. Xu, S.; Jiang, H.H.; Xiong, F.; Zhang, C.; Xie, M.J.; Li, Z.X. Evaluation for block-scale solar energy potential of industrial block and optimization of application strategies: A case study of Wuhan, China. *Sustain. Cities Soc.* **2021**, *72*, 103000. [CrossRef]
11. Shang, C. Study on the Impact of Urban Morphology at the Block Scale on Building Group Energy Consumption Based on Software Simulation. Master's Thesis, Southeast University, Dhaka, Bangladesh, 2019.
12. Mohajeri, N.; Upadhyay, G.; Gudmundsson, A.; Assouline, D.; Kämpf, J.; Scartezzini, J.L. Effects of urban compactness on solar energy potential. *Renew. Energy* **2016**, *93*, 469–482. [CrossRef]
13. Ye, Q.; Zhang, X.Z.; Zhao, Q.; Li, X.Y. Analysis of Factors Influencing the Scale of Urban Residential Blocks. *Urban Plan.* **2019**, *43*, 78–84.
14. Zhang, W. Research on Photovoltaic Applications in the Built Environment. Master's Thesis, Tianjin University, Tianjin, China, 2018.
15. Wang, J. Design Optimization of Commercial Shared Spaces Based on "Environmental Regulation" Guidance. Master's Thesis, China Academy of Building Research, Beijing, China, 2024.
16. Qin, H.Z. Research on Low-Carbon Renewal Strategies for Old Urban Communities in Cold Regions Based on Carbon Emission Models. Master's Thesis, Shandong Jianzhu University, Shandong, China, 2024.
17. Chatzipoulka, C.; Compagnon, R.; Nikolopoulou, M.J.S.E. Urban geometry and solar availability on façades and ground of real urban forms: Using London as a case study. *Sol. Energy* **2016**, *138*, 53–66. [CrossRef]

18. Li, Z.W.; Quan, S.J.; Yang, P.P.J. Energy performance simulation for planning a low carbon neighborhood urban district: A case study in the city of Macau. *Habitat Int.* **2016**, *53*, 206–214. [CrossRef]
19. Wang, M.; Ren, Y.C.; Zhang, B.Q.; Gao, X.C.; Xu, H.; Ji, G.H.; Ma, Q. Research on Passive Energy-saving Renovation of Residential Buildings in Western Inner Mongolia—A Case Study of Ordos. *Build. Energy Effic.* **2024**, *52*, 87–93.
20. *GB 50797-2012*; Design Specification for Photovoltaic Power Plants. China Planning Press: Beijing, China, 2012.
21. Zheng, F.; Wang, Y.; Shen, Z.; Wang, Y. Research on the Correlations between Spatial Morphological Indices and Carbon Emission during the Operational Stage of Built Environments for Old Communities in Cold Regions. *Buildings* **2023**, *13*, 2222. [CrossRef]